



ISSN (E): 2277-7695
ISSN (P): 2349-8242
NAAS Rating: 5.23
TPI 2022; SP-11(10): 1043-1053
© 2022 TPI

www.thepharmajournal.com

Received: 05-07-2022

Accepted: 09-08-2022

Dr. Adarsh M. Kalla
Southern Regional Station,
ICAR-National Dairy Research
Institute, Bengaluru, Karnataka,
India

Dr. Magdaline Eljeeva Emerald Franklin
Southern Regional Station,
ICAR-National Dairy Research
Institute, Bengaluru, Karnataka,
India

Heartwin A. Pushpadassa
Southern Regional Station,
ICAR-National Dairy Research
Institute, Bengaluru, Karnataka,
India

Sathish Kumar M.H.
Southern Regional Station,
ICAR-National Dairy Research
Institute, Bengaluru, Karnataka,
India

Surendra Nath Battula
Southern Regional Station,
ICAR-National Dairy Research
Institute, Bengaluru, Karnataka,
India

Corresponding Author:
Dr. Adarsh M. Kalla
Southern Regional Station,
ICAR-National Dairy Research
Institute, Bengaluru, Karnataka,
India

Isolation and characterization of cellulose from coconut shell powder and its reinforcement in casein films

Dr. Adarsh M. Kalla, Dr. Magdaline Eljeeva Emerald Franklin, Heartwin A. Pushpadassa, Sathish Kumar M.H. and Surendra Nath Battula

Abstract

Cellulose was extracted from coconut shell powder (CSP) as a source of natural fiber, and used as reinforcing material in casein composite films. Extraction was done by delignification and mercerization of CSP. The microfibers structural and surface analyses revealed that their diameter had decreased and showed changes in surface morphology from that of the raw fibres. This has been further confirmed by SEM, XRD and FTIR results. The cellulose prepared in this work has been shown to possess good flow properties compared to CSP and commercial cellulose. The reinforcing capacity of 3% cellulose was evaluated in casein films prepared by casting method. Casein composite films with added cellulose increased their tensile strength and elastic modulus. However, the tensile strain decreased after incorporation of cellulose, indicating good toughness and resistance to deformation.

Keywords: Casein composite film, cellulose, characterization, coconut shell powder, film properties

1. Introduction

Natural fibers used as fillers/reinforcements in composite films has increased tremendously in recent times as they are environment friendly and shown to improve the film properties (Satyanarayana, Arizaga, & Wypych, 2009) [32]. Apart from being biodegradable, the natural fibers are cost effective and renewable, possess low density, high tensile strength and release negligible CO₂ emissions. The natural fiber-reinforced composites are not a suitable replacement for synthetic polymers in every packaging application because of their limitations such as poor compatibility with other polymer matrices and hydrophilicity in composites but can be used as single-use packaging material (John & Anandjiwala, 2008; Deka, Misra, & Mohanty, 2013; Majeed *et al.*, 2013) [19, 11, 23]. Adhesion of natural fibers with other polymer matrices could be improved and their moisture uptake could be reduced through chemical treatments such as benzylation, acetylation, acrylation, alkalization and silane treatment. These treatments modify the hydroxyl groups in natural fibers that impart hydrophilicity (John & Anandjiwala, 2008) [19].

Natural fibers obtained from plant and cellulose-based sources are common bio-fillers for reinforcing polymer matrices (Singha & Thakur, 2009) [35]. Notably, quality fibrous fillers can be obtained from agricultural wastes such as bagasse, wheat straws, rice husks, groundnut shells, coconut husk and cotton stalks (Thakur, Thakur, & Gupta, 2014) [42]. Wood and cotton are the principal sources for cellulose, a natural fiber. Coconut shell contains lignin, hemicellulose and cellulose, which possess good thermo-stability (Mantia, Morreale, & Ishak, 2005) [24]. It is available in abundance in the tropical countries, wherein 90% of them are disposed as waste, used as fuel or burnt in open air (Madakson, Yawas, & Apasi, 2012) [22]. Cellulose could be extracted from agricultural wastes such as coconut shell by removing the non-cellulosic constituents by delignification and mercerization. Hence, coconut shell powder (CSP) can be a good source for obtaining cellulosic fibers for manufacturing of composites (Sarki, Hassan, Aigbodion, & Oghenevweta, 2011) [31].

Cellulose is a straight chain semi-crystalline polymer of D-glucopyranose units with no branching of the molecular chains. In most agricultural sources, it is available as a composite material along with other components as lignocellulose, hemicellulose, etc. The chemical structure of cellulose is similar to that of starch. However, due to the $\beta(1\rightarrow4)$ glycosidic bonds that exist within, cellulose makes it extremely rigid. Each unit of cellulose contains three hydroxyl groups associated with hydrogen bonds to form bundles of fibrils, wherein highly ordered crystalline regions alternate with disordered amorphous regions (Bodirlau, Teaca, & Spiridon, 2013) [7].

Due to its fibrous nature, cellulose as a bio-filler can align and orient itself uniaxially enhancing its mechanical strength (Haafiz *et al.*, 2013) [16], flexibility, biocompatibility, thermal and chemical stability (Hahary, Husseinsyah, & Zakaria, 2016) [17]. The utilization of cellulose as reinforcement in thermoplastic matrices was demonstrated by several researchers (Haafiz *et al.*, 2013; Teacă, Bodirlău, & Spiridon, 2013; Hahary *et al.*, 2016; Sudharsan *et al.*, 2016) [16, 41, 17, 38]. Similarly, addition of 15% (w/w) cellulose to starch-based films improved their water resistance (Dufresne & Vignon, 1998) [12].

Casein is a unique milk protein with random coil structure, and possess excellent film-forming properties due to the lack of secondary structure and presence of weak intermolecular electrostatic, hydrophobic and hydrogen bond interactions (McHugh & Krohta, 1994) [25]. It tends to form transparent and flexible films because the presence of hydroxyl and amino groups in casein provides good oxygen barrier property to the films (Bonnaillie, Zhang, Akkurt, Yam, & Tomasula, 2014) [8]. Since casein has polar groups, it can be used in combination with other polymers (fat based polymers) in order to protect products that are prone to oxidation. However, due to the presence of hydrophilic groups, these films have poor mechanical and moisture barrier properties, which could be circumvented to a large extent by incorporation of cellulosic fibers as reinforcing agent.

This study aims to produce packaging films from natural biopolymers such as casein and cellulose. Cellulose was extracted from CSP as there have been few attempts to extract it from this cheap source. The objective was to improve the mechanical and water vapor barrier properties of casein films by incorporation of cellulose fibers extracted from CSP. The improvement in mechanical and water vapor barrier properties of casein films after reinforcement with cellulosic fibers was evaluated.

2. Experimental Methods

2.1 Materials

CSP was provided by Master Micron International (Bengaluru, India), while sodium chlorite (83%, MW: 90.44), glacial acetic acid (99.6%, MW: 60.05) and sodium hydroxide (97%), commercial cellulose (source: cotton linters) were purchased from HiMedia Laboratories Pvt. Ltd. (Mumbai, India). All other chemicals used were of analytical reagent grade.

2.2 Extraction of cellulose fibers

The CSP was sieved using sieve shaker (Model: Retsch AS 200, Germany) to $\leq 63 \mu\text{m}$ for extraction of cellulose. The extraction and removal of non-cellulosic components from CSP was done by delignification and mercerization. Delignification was performed in accordance with ASTM D1104-56 (1978) [4] to primarily remove lignin. The CSP was washed with warm water at 50 °C to remove the impurities, and dried at 70 °C for 2 h. It was bleached by acidified sodium chlorite solution, with pH adjusted to 3-4 by glacial acetic acid at 70 °C for 5 h to remove lignin. The cellulose obtained was referred to as 'holocellulose', which was filtered, washed and rinsed with distilled water. The holocellulose was further treated with aqueous solution of 5% NaOH for 2 h at ambient temperature to produce cellulose according to ASTM D1103-60 (1977) [3]. The solution was filtered, washed with distilled water and oven-dried at 70°C for 8 h. The cellulose yield was expressed as percentage of

CSP used (Eq. 1).

$$\text{Yield (\%)} = \frac{W_f}{W_i} \times 100 \quad (1)$$

Where, 'W_i' is the initial weight of CSP and 'W_f' is the final dried weight of extracted cellulose.

2.3 Moisture content

Exactly 3 g of CSP was spread in a Petri plate and oven-dried at 105 °C for 24 h. (Ilyas, Sapuan, & Ishak, 2017) [18]. It was transferred to a desiccator, cooled and weighed to estimate the moisture content (Eq. 2). The moisture contents of extracted and commercial celluloses were similarly estimated.

$$\text{Moisture content} = \frac{M_i - M_f}{M_i} \times 100 \quad (2)$$

Where, 'M_i' is the initial weight of sample and 'M_f' is the final dried weight.

2.4 Optical microscopy

The structure of CSP, extracted cellulose and commercial cellulose was observed using an optical microscope (Model: Nikon YS200, Minato, Tokyo, Japan). A drop of suspension prepared using distilled water was spread on the glass slide, stained with methylene blue to obtain adequate contrast, and images were acquired at 100X and 400X magnifications.

2.5 Scanning electron microscopy-energy dispersive X-ray spectroscopy

The morphology of extracted and commercial celluloses was examined by scanning electron microscopy (SEM) (Model: Ultra 55, Zeiss, Jena, Germany). The samples were sputter-coated with 5-10 nm gold to make them conductive, and were observed under 10⁻⁵ mbar vacuum with accelerating voltage of 5 kV. Energy dispersive X-ray spectroscopy (EDS) was used to identify the elemental composition of celluloses. The detector used was X-Max EDS (Oxford Instruments, Oxford, UK) with Peltier cooling.

2.6 Atomic force microscopy

The morphology and surface roughness of cellulose extracted from CSP was determined using atomic force microscope (AFM) (Model: ScanAsyst, Bruker, Santa Barbara, USA). Samples were prepared by dispersing 100 mg of cellulose in 10 mL deionized water, and the mixture was ultrasonicated for 8-10 min. Exactly 20 μL of the mixture was drop-casted on a clean slide and dried for 36 h under vacuum. The morphology and topography of cellulose were analyzed using 2-D and 3-D images.

2.7 X-ray diffractometry

The X-ray diffraction (XRD) was used to examine the crystallinity of CSP and both celluloses. The samples were analyzed in the X-ray diffractometer (Model: Rigaku SmartLab, Tokyo, Japan) using Cu-K α radiation ($\lambda=0.154 \text{ nm}$) at 40 kV and 30 mA with goniometer speed of 0.02 s⁻¹. The spectra were measured for 2 θ in the range of 10-40°. The X-ray detector used was scintillation counter, with detector angle of 40°, and placed at a distance of 300 mm. The crystallinity index was calculated using Eq. (3) as suggested

by Segal, Creely, Martin Jr, and Conrad (1959)^[33].

$$\text{Crystallinity index} = \frac{I_{002} - I_{\text{am}}}{I_{002}} \times 100 \quad (3)$$

Where, 'I₀₀₂' (002 plane diffraction) is the peak intensity of the crystalline regions and 'I_{am}' is the peak intensity of amorphous region.

2.8 Fourier transform infrared spectroscopy

The Fourier transform infrared (FTIR) spectra of CSP and celluloses were recorded using the FTIR spectrometer (Model: Perkin Elmer Frontier, Singapore). The sample was finely ground, mixed with potassium bromide in the ratio of 5:95 and compressed into pellets using 5 tonne press. The

$$\text{True density } (\rho_{\text{true}}) = \frac{\text{Weight of powder (g)}}{\text{Total volume of petroleum ether with suspended powder (mL) - 28}} \quad (4)$$

2.10 Flow properties

The bulk and tapped densities of CSP and celluloses were determined as per the method given by Mitra *et al.* (2017)^[26] Briefly, 50 g of sample (W) was allowed to flow freely through a funnel into 250 mL graduated cylinder, and it was gently tapped on a wooden bench three times. The bulk volume (V_o) was recorded, and the bulk density (ρ_{bulk}) was computed using Eq. (5). For tapped density (ρ_{tapped}), the cylinder with sample was tapped 500 times using the tapped density tester (Model: Thermonik, Campbell Electronics, Mumbai, India), and the final tapped volume was recorded (V_f). The tapped density was determined using Eq. (6).

$$\text{Bulk density } (\rho_{\text{bulk}}) = \frac{W}{V_o} \quad (5)$$

$$\text{Tapped density } (\rho_{\text{tapped}}) = \frac{W}{V_f} \quad (6)$$

The Carr's index (CI) and Hausner ratio (HR) indicate the flowability and cohesiveness of powders. The CI and HR of CSP and celluloses were calculated from ρ_{bulk} and ρ_{tapped} using Eqs. (7) and (8), respectively.

$$\text{Carr's index (\%)} = \frac{\rho_{\text{tapped}} - \rho_{\text{bulk}}}{\rho_{\text{tapped}}} \times 100 \quad (7)$$

$$\text{Hausner ratio} = \frac{\rho_{\text{tapped}}}{\rho_{\text{bulk}}} \quad (8)$$

The porosity of CSP and celluloses was estimated from the ρ_{bulk} and ρ_{true} using Eq. (9).

$$\text{Porosity (\%)} = \left(1 - \frac{\rho_{\text{bulk}}}{\rho_{\text{true}}} \right) \times 100 \quad (9)$$

The static angle of repose (AoR) was measured using optical

wavenumber of the scans varied from 400 to 4000 cm⁻¹ with 32 scans per minute at the spectral resolution of 4 cm⁻¹.

2.9 True density

The true density (ρ_{true}) was calculated using the method given by Pushpadass, Emerald, Rao, Nath, and Chaturvedi (2014)^[28] Exactly 5 g of sample was taken in 50 mL centrifuge tube and 25 mL of petroleum ether was added to it. The tube was closed with an air-tight stopper. The sample contained in the tube was vortexed for 1 minute to ensure that all particles were evenly dispersed. Again 3 mL of petroleum ether was used to wash the powder particles sticking to the walls of the tube, and the contents were vortexed for 5 min. The total volume of petroleum ether along with suspended powder was read, and true density was calculated using Eq. (4).

imaging method. Both cellulose powders were allowed to pass through a fixed funnel to form a free-standing pile on a plane surface. The images of the sample pile were captured using a digital camera. The AoR was computed from the images using the "DropSnake" plugin of ImageJ software ver. 1.45 (National Institutes of Health, Bethesda, MD) after converting them into gray-scale (Mitra *et al.*, 2017)^[26].

2.11 Reinforcing ability of isolated cellulose fibers

The reinforcing capacity of extracted cellulose was assessed in casein films prepared by casting (Wagh, Pushpadass, Emerald, & Nath, 2014)^[28]. The film forming solution was prepared by dissolving 18 g of casein in 200 mL of warm distilled water, whose pH was adjusted to 5.6 using 2 N NaOH solution. The cellulose was added as reinforcing agent at 3%, maintaining the total solids content in the film-forming solution at 9%. The solution was heated on a hot plate at 85°C with constant stirring for 15 min. Glycerol was added as plasticizer at 0.25% (w/w) of solution, while potassium sorbate at 0.2% (w/w) of biopolymer was added as antimicrobial agent. Heating was continued for 5 min and the solution was cooled to 40-45 °C, and poured onto glass molds of 290×200×4 mm size lined with polytetrafluoroethylene (PTFE) sheet. The film-forming solutions were dried at 40°C for 96 h. After drying, the films were peeled-off from the molds and equilibrated at 27 °C and 65% RH for 48 h in a desiccator containing saturated potassium iodide solution before testing.

The thickness of cast films was measured using a digital caliper (Model: CD 6"CSX, Mitutoyo Corp., Japan) at 5 random locations and the mean value was calculated. The water vapor permeability (WVP) of the films was determined using water vapor transmission rate (WVTR) estimated gravimetrically using wet cup method (ASTM E96-95, 1995)^[5]. The film specimen of 8×8 cm was cut and mounted on polycarbonate cups filled with distilled water to 1 cm from the film underside. The lid was tightened and cup with film was then placed in stability chamber maintained at 27°C and 65% RH. The weight loss of the cup was measured at 2 h interval and the steady state portion of the weight loss (up to 12 h) versus time curve was used to compute the WVTR. The WVP was computed using Eq. (10).

$$WVP = \frac{WVTR \times t}{\Delta p} \tag{10}$$

Where, ‘t’ is mean thickness of film specimen and ‘Δp’ is water vapor partial pressure difference (kPa) between the two sides of specimen. Each film was analyzed three times and the mean WVP was computed.

The tensile properties of the films were analyzed using the texture analyzer (Model: TA.XT Plus, Stable Micro Systems, Godalming, Surrey, UK). Strips of 2.5×15 cm were cut, and were fixed onto the jaws of A/TG tensile grips. The distance between the grips was kept at 100 mm, and the film strips were tested at the speed of 0.5 mm/s until they break. Tensile strength, Young’s modulus and elongation at break were determined with eight replications.

3. Results and Discussion

3.1 Extraction and yield of cellulose

The CSP obtained after sieving had a particle size of ≤63 μm, and was dark brown in color due to the presence of hemicellulose and lignin. The progressive removal of hemicellulose or lignin and consequent increase in cellulose content of CSP can be judged by the change in color after each successive treatment (Fig. 1). Delignification changed the color of CSP from dark brown to off white as lignin was removed. Further alkali treatment showed more evident color change, and the powder exhibited the characteristic whiteness of cellulose. From the color changes, it is evident that delignification was effective in removing non-cellulosic components such as lignin, hemicellulose and waxes from CSP. After delignification and alkali treatment (mercerization), about 30% of lignin and 42.5% of hemicellulose were removed, and the final cellulose yield was about 27.5% of the initial weight of CSP. The results obtained were in agreement with the yield of cellulose reported by Liyanage and Pieris (2015)^[21].

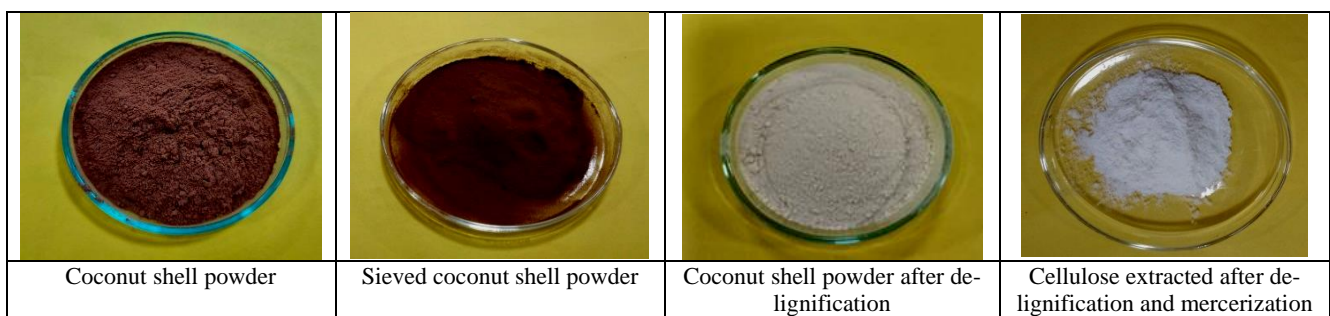


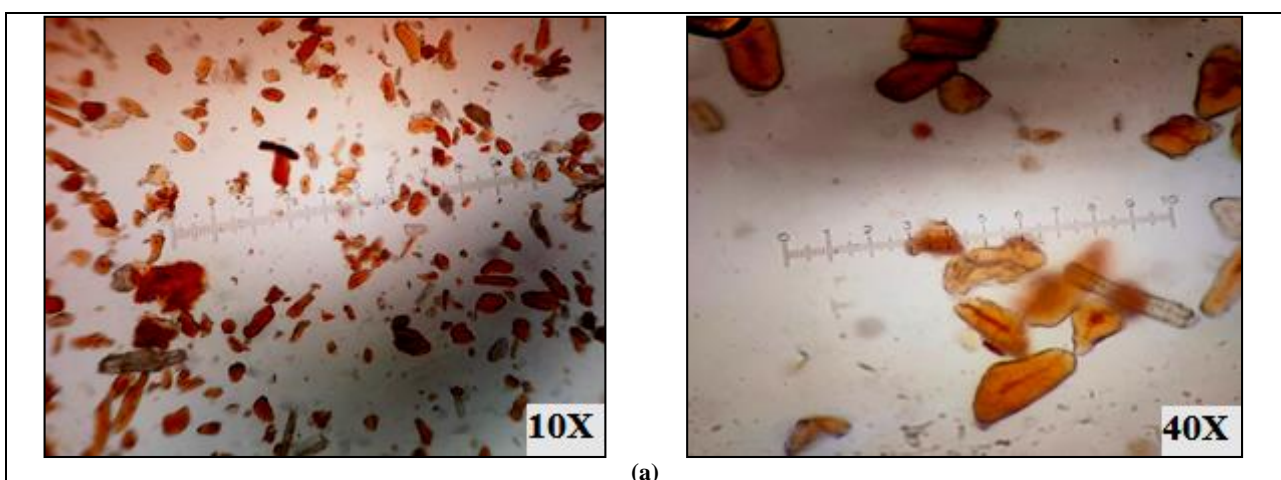
Fig 1: Cellulose extracted from coconut shell powder

3.2 Moisture content

The moisture content of cellulose fibers is an important characteristic while selecting it as filler in polymer composite films. Fiber with lower moisture content would be preferable as filler in bio-composites because higher moisture could reduce the tensile strength and lead to pore formation in the films (Razali, Salit, Jawaid, Ishak, & Lazim, 2015; Jumaidin, Sapuan, Jawaid, Ishak, & Sahari, 2017)^[30, 20]. The moisture content of CSP was 4.9%, while it was much less at 2.5% and 3.7% for extracted and commercial cellulose, respectively.

3.3 Optical microscopy

The particle size of CSP reduced considerably after sieving as seen from the light microscopic images (Figs. 2a and b). The cellulose fibers obtained after chemical treatment decreased in diameter because they became fibrillated due to the disruption of internal structure of CSP when non-cellulosic materials were removed by delignification and mercerization. Collazo-Bigliardi, Ortega-Toro, and Boix (2018)^[9] also observed similar reduction in diameter of cellulose extracted from coffee and rice husk after chemical treatment.



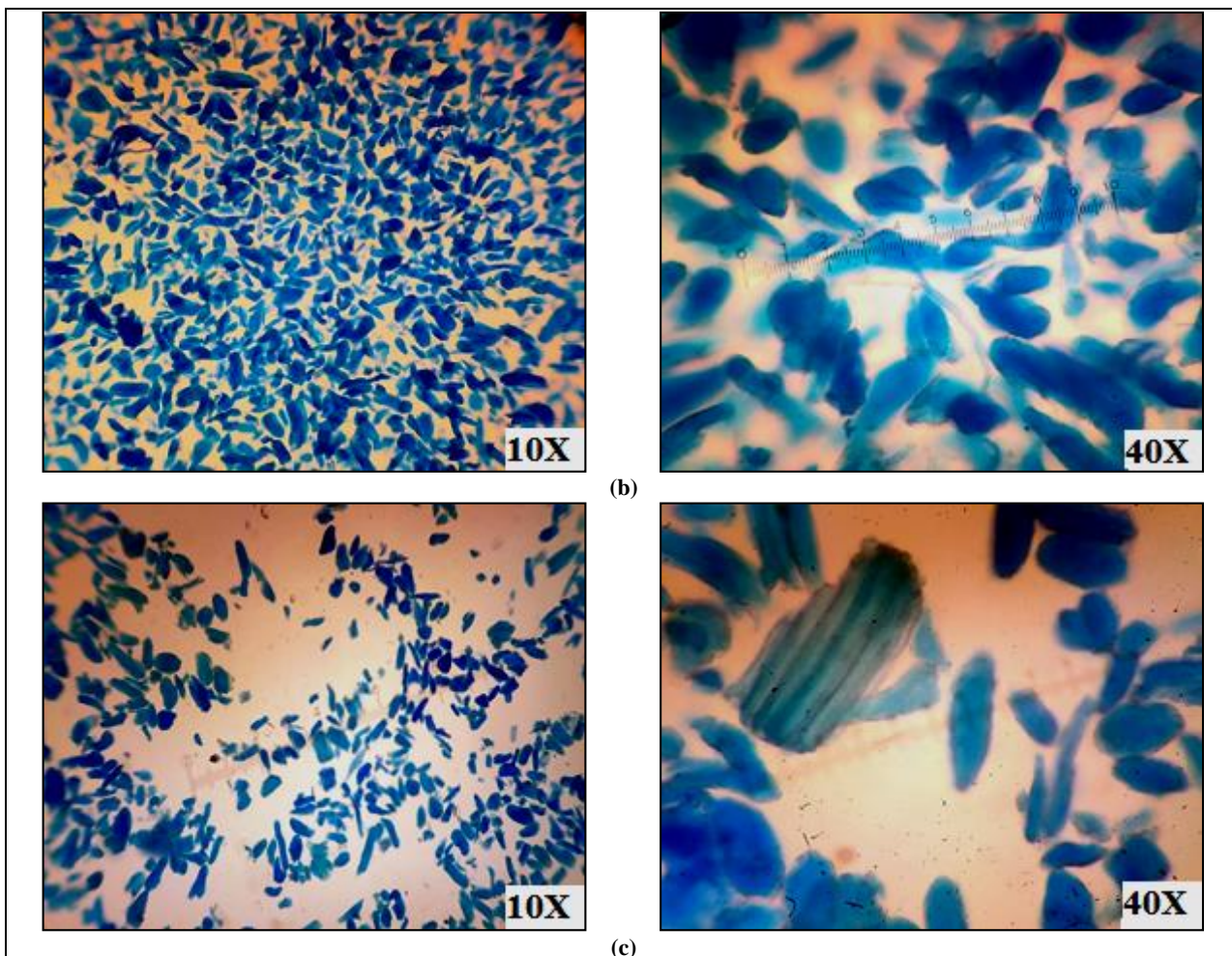


Fig 2: Optical microscopic images of (a) coconut shell powder (b) extracted cellulose and (c) commercial cellulose

3.4. Scanning electron microscopy

The SEM micrographs showed that the chemical treatment during extraction reduced the size of cellulose fibers from 63 μm to 5-20 μm (Fig. 3). The diameter of CSP reduced because the composite fibril structure was broken into individual cellulose micro-fibrils after the removal of lignin and hemicellulose. The empty space between the fibers (Fig. 3a) was indicative of the removal of non-cellulosic materials such as lignin, hemicellulose and waxes. The SEM image of commercial cellulose (Fig. 3b) also shows the presence of fibers in it. The diameter of cellulose obtained from CSP was similar in size to the cellulosic fibers of banana (10 μm)

(Deepa *et al.*, 2011) [10], kneaf (13 μm) (Tawakkal, Talib, Abdan, & Ling, 2012) [40], hibiscus sabdariffa (10.4 μm) (Sonia & Dasan, 2014) [37], and oat husk (10-45 μm) (Qazanfarzadeh & Kadivar, 2016) [29].

The EDS spectrum of both extracted and commercial cellulose showed the peaks of carbon, oxygen and nitrogen, and their elemental composition as well (Fig. 4). The carbon and oxygen content were to the extent of 34.84% and 46.08%, respectively. The extracted cellulose also contained small amounts of impurities such as sodium at 0.54% and chlorine at 0.42%.

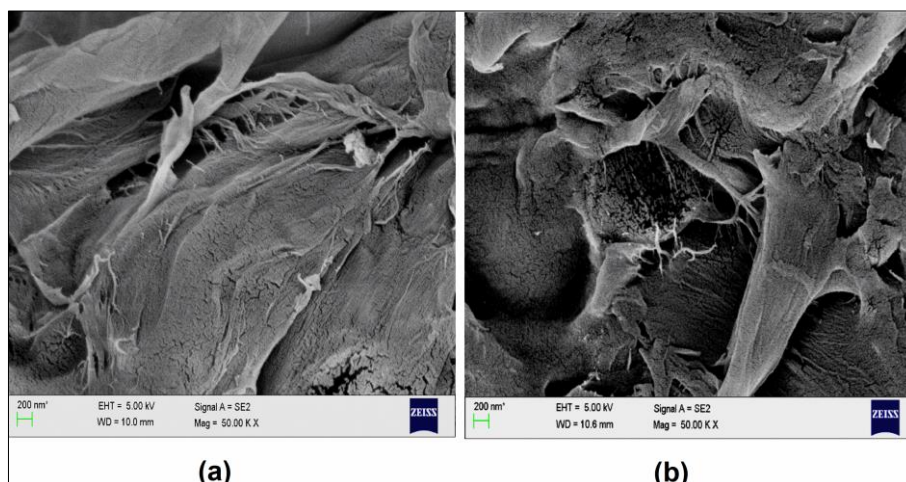


Fig 3: Scanning electron micrographs of (a) cellulose extracted from CSP and (b) commercial cellulose microfibrils

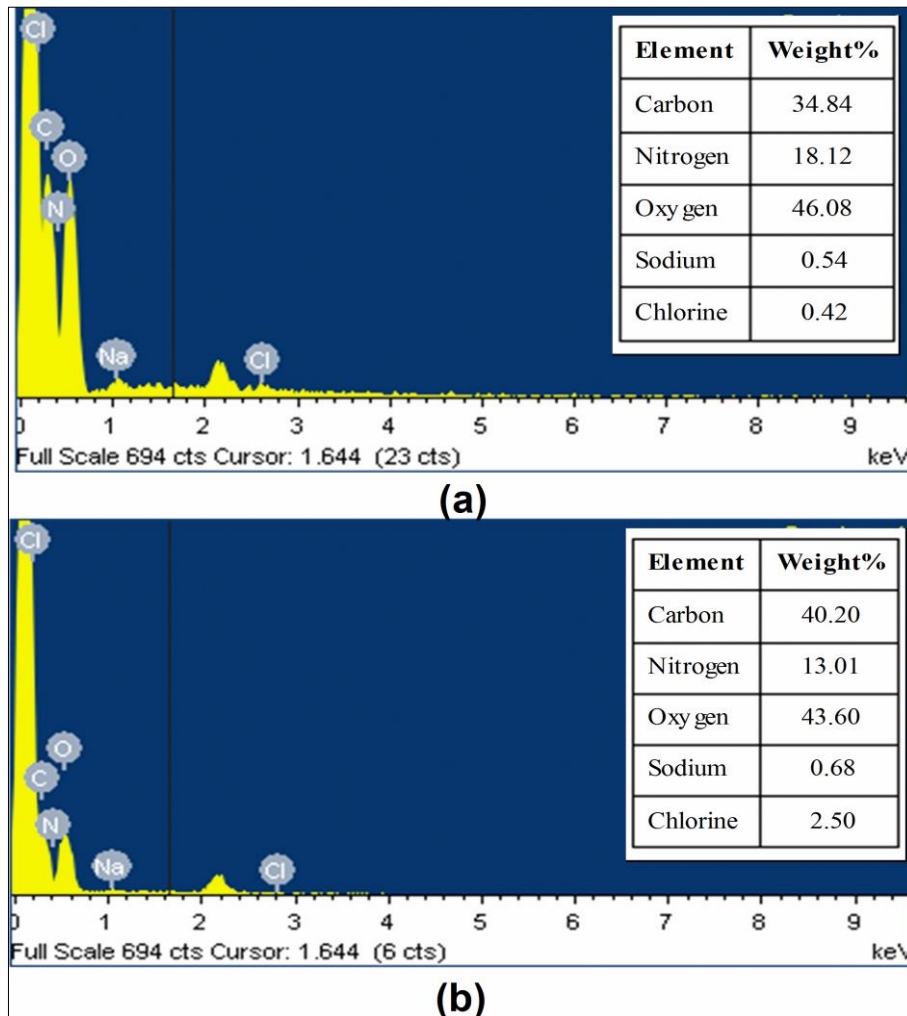


Fig 4: Energy dispersive X-ray spectrum of (a) extracted cellulose and (b) commercial cellulose

3.5. Atomic force microscopy

The AFM topography of cellulose extracted from CSP is depicted in Fig. 5. The 2D image (Fig. 5a) shows aggregated structures with high surface area, which would support better interaction between casein and cellulose during processing into composite films. The 3D image (Fig. 5b) of extracted

cellulose consisted of spherical particles with non-uniform and rough surfaces, with mean surface roughness of 1.37 nm. From Fig. 5a, it can be observed that cellulose contained both brighter and darker regions, representing crystalline and amorphous regions, respectively.

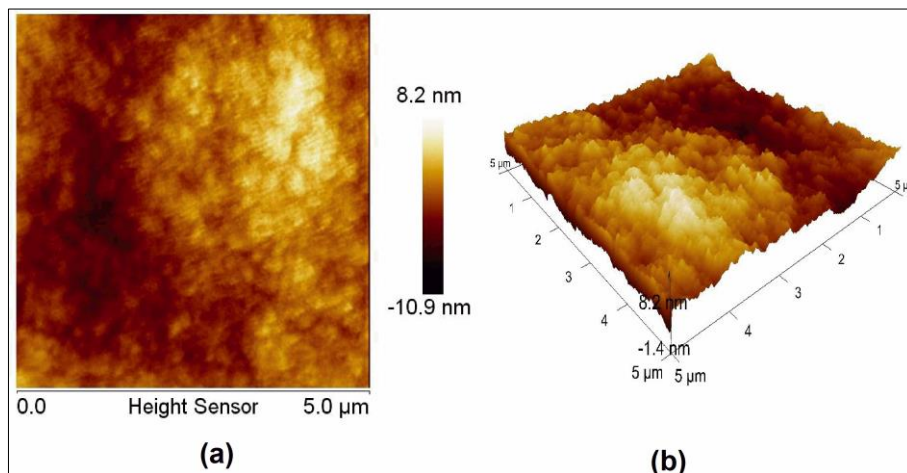


Fig 5: 2D (a) and 3D (b) atomic force microscopic images of extracted cellulose

3.6. X-ray diffractometry

Crystallinity is an important property that influences the mechanical properties of fibers. The X-ray diffractograms of CSP, extracted and commercial celluloses are shown in Fig. 6. The diffractograms (Fig. 6) of CSP, extracted and commercial celluloses displayed sharp peaks (I_{002}) at 2θ of 22.10° , 22.48° and 22.47° , respectively. The steep and intense I_{002} peak of extracted and commercial celluloses was typical of their higher crystalline content. The shoulder peak (I_{am}) of CSP, extracted cellulose and commercial cellulose was observed at 2θ of 16.46° , 17.82° and 18.35° , respectively. This indicated the dissolution of lignin and hemicellulose during chemical

treatment. After non-cellulosic components were removed by delignification and mercerization, the crystallinity index noticeably increased from 47.8% in CSP to 65.9% in extracted cellulose. In comparison, commercial cellulose had much higher crystallinity index of 77.7%. The reduction in crystalline content in extracted cellulose and the additional peaks observed in the diffractogram were due to the ability of fibrils to rearrange themselves into less dense and rigid interfibrillar regions and develop newer crystalline regions (Gassan & Bledzki, 1999) [15]. Sofla, Brown, Tsuzuki, and Rainey (2016) [36] reported crystallinity index of 65% for cellulose extracted from bagasse.

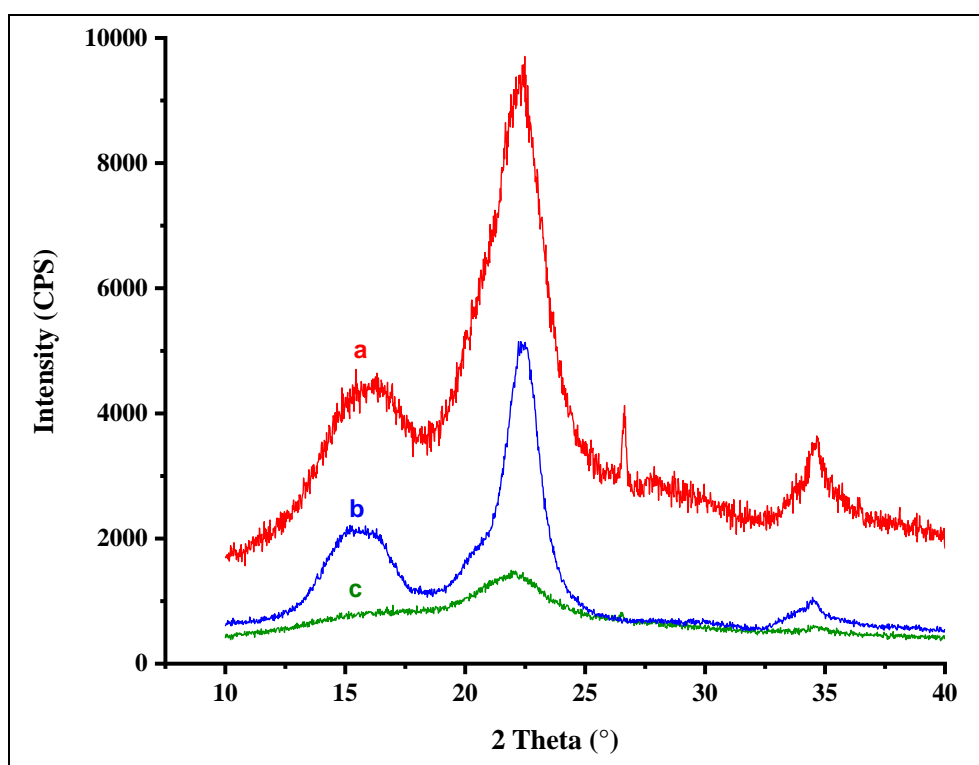


Fig. 6 X-ray diffraction patterns of (a) extracted cellulose (b) commercial cellulose and (c) coconut shell powder

3.7 Fourier transform infrared spectroscopy

The FTIR spectra of CSP, extracted and commercial celluloses are shown in Fig. 7 & 8 and Table 1. The typical bands of raw CSP were observed at 1740 , 1608 , 1511 , 1458 , 1247 and 1119 and 1010 cm^{-1} . In these, the bands at 1458 and 1247 cm^{-1} were due to lignin. The peaks at 1608 and 1511 cm^{-1} represented the C=C stretching vibrations of the aromatic ring of lignin (Qazanfarzadeh & Kadivar, 2016) [29], while the peak at 1458 cm^{-1} was assigned to CH_3 bending and at 1247 cm^{-1} was ascribed to C=O out-of-plane stretching vibrations of aryl group. These peaks completely disappeared in extracted cellulose after chemical treatment (also absent in commercial cellulose), indicating successful removal of lignin from the fibers. The band observed at 1740 cm^{-1} in CSP was ascribed to C=O stretching of acetyl and uronic ester groups of hemicellulose. The absence of this band in extracted and commercial celluloses also corroborates the removal of hemicellulose by chemical treatment.

The broad absorption peak in the 3400 - 3100 cm^{-1} region,

representing O-H groups, was common to the spectrum of CSP, extracted and commercial celluloses (Fig. 7). However, the peak was relatively broader for CSP, which was suggestive of the higher number of OH groups due to its higher moisture content. In the spectrum of extracted cellulose, the peaks at 2900 and 1651 cm^{-1} wavenumbers were attributed respectively to the asymmetric stretching of C-H groups and stretching of O-H groups, representing adsorbed water (Shen, Ghasemlou & Kamdem, 2015) [34], while the peak at 1431 cm^{-1} was assigned to the bending of CH_2 groups of cellulose. Similarly, the peaks at 1375 , 1320 , 1058 , 1157 and 1032 cm^{-1} reflected the C-H₂ deformation vibration, C-H₂ rocking vibration, C-O-C pyranose ring skeletal vibration, C-O-C asymmetric valance vibration and C-O stretching vibration, respectively. The peak at 896 cm^{-1} is the characteristic of the β -(1 \rightarrow 4) linked glycosidic bonds in cellulose. The typical peaks related to lignin and hemicellulose were absent in the extracted cellulose.

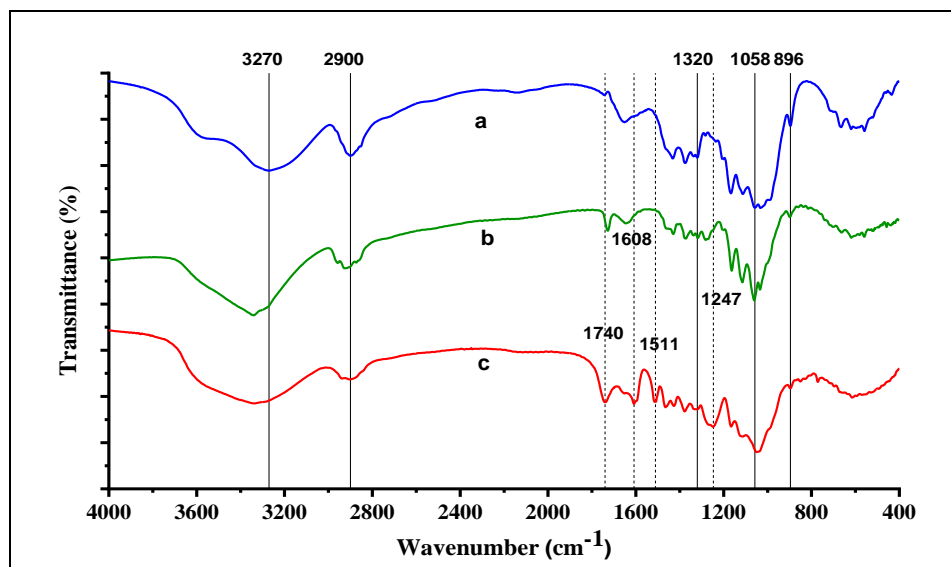


Fig. 7 Fourier transform infrared spectra (400 to 4000 cm^{-1} wavenumber) of (a) extracted cellulose (b) commercial cellulose and (c) coconut shell powder

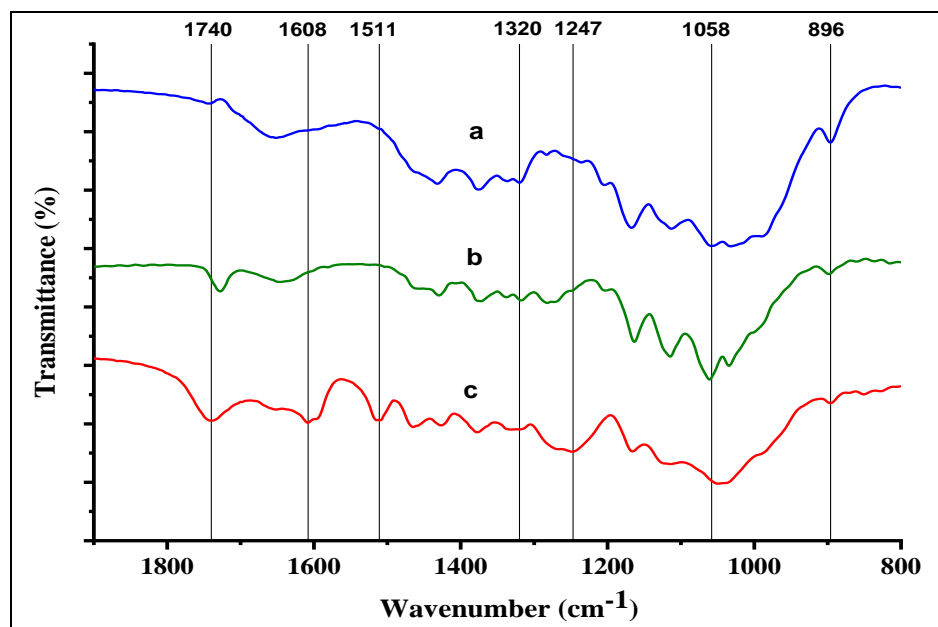


Fig. 8 Fourier transform infrared spectra (800 to 1900 cm^{-1} wavenumber) of (a) extracted cellulose (b) commercial cellulose and (c) coconut shell powder

Table 1: Vibrational frequencies (cm^{-1}) of coconut shell powder and cellulose

Wavenumber (cm^{-1})	Coconut shell powder	Cellulose isolated from coconut shell powder and commercial cellulose
3400-3100	Stretching and bending bands of O-H groups in cellulose	Stretching and bending bands of O-H groups in cellulose
2900	-	Stretching of C-H groups
1740	C-O stretching of the acetyl and uronic ester groups of hemicellulose	Not present
1608	Indicates presence of lignin	Not present
1651	-	Stretching of O-H groups representing the adsorbed water in carbohydrate
1511	C=C stretching vibration in the aromatic ring of lignin	Not present
1431	-	Bending of CH_2 groups representing presence of cellulose in carbohydrate
1320	-	C-H ₂ rocking vibration
1247	Presence of lignin and represents the C-O out of plane stretching vibration of the aryl group	Not present
1058	-	C-O-C pyranose ring skeletal vibration
896	-	C-H deformation vibration

3.8 True density

The true density of CSP, extracted and commercial cellulose was 1657, 1313 and 1470 kg/m³, respectively. The true density of isolated cellulose was lower as compared to that of CSP and commercial cellulose due to the increased voids created by separation of fibrillar bundles into individual fibers during removal of lignin and hemicellulose. The alpha and beta polymorphs of crystalline cellulose have true density of 1582 and 1599 kg/m³, respectively (Sun, 2005) [39]. The closer the true density of cellulose to its crystalline counterpart, the higher is its degree of crystallinity (Achor, Oyeniyi, & Yahaya, 2014) [2].

3.9 Flow properties

The flow properties of CSP and celluloses are summarized in Table 2. The bulk and tapped densities for cellulose were in accordance with those reported for lignocellulosic fibers from peanut husk (310 and 370 kg/m³) (Azubuike, Odulaja, & Okhamafe, 2012) [6]. The bulk and tapped densities of extracted cellulose were higher than that of commercial cellulose but lower than the values of CSP. This might be due to the smaller particle size and less interparticle attractions due to its lower moisture content as compared to commercial cellulose. As moisture in commercial cellulose was higher (3.7% as compared to 2.5% for extracted cellulose), it promoted adhesion and liquid bridging between particles, leading to reduction in bulk density. In general, flowability of

a material is better if the difference between bulk and tapped densities is lower. Thus, extracted cellulose had better flow characteristics than commercial cellulose because of less interparticular adhesion and bridging interactions due to lower moisture content. Particles having low internal porosity tend to possess better flow properties. As the porosity of cellulose extracted from CSP was lower (0.71) than that of cellulose (0.79), it was expected to have better flow properties as compared to commercial cellulose.

CI of greater than 25% for CSP and celluloses suggested that they were cohesive powders with 'passable' to 'poor' flowability (Wu, Ho, & Sheu, 2001) [44]. Amongst the three samples, the HR and CI of commercial cellulose were found to be higher than that of isolated cellulose. This could be ascribed to its higher moisture content, causing difficulties to flow due to adhesion and bridging. The HR and CI data of commercial cellulose were supported by its higher value of AoR as well. AoR, a qualitative indicator of cohesive and internal friction in the powders, is presented in Table 1. In comparison to commercial grade, extracted cellulose had intermediate cohesiveness and fair level of flowability. The AoR of CSP and extracted cellulose were slightly above 40°, while that of commercial cellulose was 55.75°. The AoR of extracted cellulose lied between the theoretical minimum of 20° for uniform spheres that flow very well and the maximum of 45° for powders that flow poorly (Fowler, 2000) [14].

Table 2: Flow properties of coconut shell powder, extracted cellulose and commercial cellulose

Property	Sample		
	Coconut shell powder	Extracted cellulose	Commercial cellulose
Bulk density, kg/m ³	500.90±8.12	368.80±3.83	303.90±12.85
Tapped density, kg/m ³	682.50±6.17	493.80±4.16	452.30±3.42
True density, kg/m ³	1657.00±2	1313.00±1	1470.00±1
Hausner ratio	1.36±0.009	1.34±0.004	1.49±0.068
Carr's index (%)	26.61±0.532	25.30±0.262	32.80±3.116
Porosity	0.69±0.004	0.71±0.002	0.79±0.008
Angle of repose (deg)	43.17±0.017	44.18±0.026	55.75±0.150

3.10 Reinforcing ability of cellulose fibers

The thicknesses of casein and casein composite films were 0.224 and 0.282 mm, respectively. The thickness of composite films increased with increase in cellulose content owing to the larger particle size of cellulose. These results were in agreement with those of El Halal *et al.* (2015) [13] who reported that increase in addition of cellulose fiber extracted from barley husk increased the thickness of barley grain starch films. Qazanfarzadeh and Kadivar (2016) [29] also reported increase in film thickness with increase in the proportion of oat nanocellulose fiber in whey protein isolate (WPI) films.

The WVP and tensile properties of casein and casein composite films are summarized in Table 3. The WVP of casein and casein composite films was 7.7×10^{-10} g/m.s.Pa and 11.6×10^{-10} g/m.s.Pa, respectively. The WVP is affected by the hydrophilic or hydrophobic nature of materials, film manufacturing process, the type, amount and distribution of additives applied, presence of voids and cracks, and final arrangement in polymer structure. The increase in WVP of composite films could be due to the rough surface of cellulose, which might have caused minor cracks or discontinuities in the casein network of the film (Abdulkhani, Hosseinzadeh, Ashori, Dadashi, & Takzare, 2014) [1]. With increase in addition of cellulose, the film microstructure

changed, while the non-reinforced films exhibited smooth and homogeneous structure. The increase in WVP with addition of cellulose could be due to the strong affinity to materials containing hydroxyls (water), which led to swelling of cellulose at higher relative humidity and causing disruption of structural network in the films (Pereda, Amica, Rácz, & Marcovich, 2011) [27]. Abdulkhani *et al.* (2014) [1] also reported similarly that addition of nanocellulose fibers to polylactic acid film effected increase in WVP.

The tensile strength and Young's modulus of casein film were 4.98 and 9.91 MPa, respectively, which increased to 7.20 and 83.42 MPa for casein composite films containing extracted cellulose. The improvement in mechanical properties after addition of cellulose was due to good dispersion and interactions between casein and cellulose via strong hydrogen bonds. The elongation at break of casein film was 52.08%, whereas it decreased to 8.66% for casein composite films containing 3% cellulose presumably due to the rigidity of cellulose fibers. Thus, casein composite films containing extracted cellulose were stiffer and harder. The results of film properties were in accordance with those of corn starch-based composites (Haafiz *et al.*, 2013) [16], WPI/nanocellulose films (Qazanfarzadeh & Kadivar, 2016) [29] and microcrystalline cellulose-reinforced tamarind seed starch films (Sudharsan *et al.*, 2016) [38].

4. Conclusions

The process to extract cellulose from CSP by chemical treatment was standardized. The optical and SEM images of extracted cellulose showed a drastic reduction in fiber diameter as compared to CSP because the composite fibril structure was broken into individual cellulose micro-fibrils after removal of lignin and hemicellulose. The absence of lignin and hemicellulose in extracted cellulose was confirmed from FTIR spectra and XRD diffractograms. The extracted cellulose had crystallinity index of 65.9%, and had intermediate cohesiveness and better flowability as compared to commercial cellulose. Incorporation of cellulose as reinforcing fibers in casein improved the mechanical properties of the composite films considerably. From the tensile strength and Young's modulus data, it could be concluded that cellulose isolated from CSP had the potential as reinforcement fiber for the production of composite films. Application of composite films for food packaging helps to realize the potential of agricultural wastes as biopolymers and reduce pollution.

5. Acknowledgements

The authors thank the Director, ICAR-National Dairy Research Institute for the financial support. The authors are also grateful to CeNSE, Indian Institute of Science, Bengaluru for their technical assistance for major analytical tests of the samples.

6. References

- Abdulkhali A, Hosseinzadeh J, Ashori A, Dadashi S, Takzare Z. Preparation and characterization of modified cellulose nanofibers reinforced polylactic acid nanocomposite. *Polymer Testing*. 2014;35:73-79.
- Achor M, Oyeniyi YJ, Yahaya A. Extraction and characterization of microcrystalline cellulose obtained from the back of the fruit of *Lagenaria siceraria* (water gourd). *Journal of Applied Pharmaceutical Science*, 2014;4(1):57-60.
- ASTM. D1103-60 Method of test for alpha-cellulose in wood, American Society for Testing and Materials, USA; c1977.
- ASTM. D1104-56 Method of test for holocellulose in wood, American Society for Testing and Materials, USA; c1978.
- ASTM E96-95. Standard test methods for water vapour transmission of materials, American Society for Testing and Materials, USA; c1995.
- Azubuiké CP, Odulaja J, Okhamafe AO. Physicotechnical, spectroscopic and thermogravimetric properties of powdered cellulose and microcrystalline cellulose derived from groundnut shells. *Journal of Excipients and Food Chemistry*. 2012;3(3):106-115.
- Bodirlau R, Teaca CA, Spiridon I. Influence of natural fillers on the properties of starch-based biocomposite films. *Composites Part B: Engineering*. 2013;44(1):575-583.
- Bonnaillie LM, Zhang H, Akkurt S, Yam KL, Tomasula PM. Casein films: The effects of formulation, environmental conditions and the addition of citric pectin on the structure and mechanical properties. *Polymers*. 2014;6(7):2018-2036.
- Collazo-Bigliardi S, Ortega-Toro R, Boix AC. Isolation and characterisation of microcrystalline cellulose and cellulose nanocrystals from coffee husk and comparative study with rice husk. *Carbohydrate Polymers*. 2018;191:205-215.
- Deepa B, Abraham E, Cherian BM, Bismarck A, Blaker JJ, Pothan LA, *et al.* Structure, morphology and thermal characteristics of banana nano fibers obtained by steam explosion. *Bioresource Technology*. 2011;102(2):1988-1997.
- Deka H, Misra M, Mohanty A. Renewable resource based "all green composites" from kenaf biofiber and poly (furfuryl alcohol) bioresin. *Industrial Crops and Products*. 2013;41:94-101.
- Dufresne A, Vignon MR. Improvement of starch films performances using cellulose microfibrils. *Macromolecules*. 1998;31(8):2693-2696.
- El Halal SLM, Colussi R, Deon VG, Pinto VZ, Villanova FA, Carreño NLV, *et al.* Films based on oxidized starch and cellulose from barley. *Carbohydrate Polymers*. 2015;133:644-653. <https://doi.org/10.1016/j.carbpol.2015.07.024>.
- Fowler HW. Powder flow and compaction. In C.J.S. Carter (Ed), *Cooper and Gunn's tutorial pharmacy*; c2000. p. 211-233.
- Gassan J, Bledzki AK. Possibilities for improving the mechanical properties of jute/epoxy composites by alkali treatment of fibres. *Composites Science and Technology*. 1999;59(9):1303-1309.
- Haafiz MM, Hassan A, Zakaria Z, Inuwa IM, Islam MS, Jawaid M. Properties of polylactic acid composites reinforced with oil palm biomass microcrystalline cellulose. *Carbohydrate Polymers*. 2013;98(1):139-145.
- Hahary FN, Husseinsyah S, Zakaria MM. Improved properties of coconut shell regenerated cellulose biocomposite films using butyl methacrylate. *BioResources*. 2016;11(1):886-898
- Ilyas RA, Sapuan SM, Ishak MR, Zainudin ES. Effect of delignification on the physical, thermal, chemical, and structural properties of sugar palm fibre. *BioResources*. 2017;12(4):8734-8754.
- John MJ, Anandjiwala RD. Recent developments in chemical modification and characterization of natural fiber-reinforced composites. *Polymer Composites*. 2008;29(2):187-207.
- Jumaidin R, Sapuan SM, Jawaid M, Ishak MR, Sahari J. Effect of seaweed on mechanical, thermal, and biodegradation properties of thermoplastic sugar palm starch/agar composites. *International Journal of Biological Macromolecules*. 2017;99:265-273.
- Liyanage CD, Pieris M. A physico-chemical analysis of coconut shell powder. *Procedia Chemistry*. 2015;16:222-228.
- Madakson PB, Yawas DS, Apasi A. Characterization of coconut shell ash for potential utilization in metal matrix composites for automotive applications. *International Journal of Engineering Science and Technology*. 2012;4(3):1190-1198.
- Majeed K, Jawaid M, Hassan AABAA, Bakar AA, Khalil HA, Salema AA, *et al.* Potential materials for food packaging from nanoclay/natural fibres filled hybrid composites. *Materials & Design*. 2013;46:391-410.
- Mantia FPL, Morreale M, Ishak ZM. Processing and mechanical properties of organic filler-polypropylene composites. *Journal of Applied Polymer Science*. 2005;96(5):1906-1913.
- McHugh TH, Krochta JM. Milk-protein-based edible

- films and coatings. *Food Technology*, 1994;48:97-103.
26. Mitra H, Pushpadass HA, Franklin MEE, Ambrose RK, Ghoroi C, Battula SN. Influence of moisture content on the flow properties of basundi mix. *Powder Technology*. 2017;312:133-143.
27. Pereda M, Amica G, Rácz I, Marcovich NE. Structure and properties of nanocomposite films based on sodium caseinate and nanocellulose fibers. *Journal of Food Engineering*. 2011;103(1):76-83.
28. Pushpadass HA, Emerald FME, Rao KJ, Nath BS, Chaturvedi B. Prediction of shelf life of gulabjamun mix using simulation and mathematical modeling-based on moisture gain. *Journal of Food Processing and Preservation*. 2014;38(4):1517-1526. <https://doi.org/10.1111/jfpp.12111>.
29. Qazanfarzadeh Z, Kadivar M. Properties of whey protein isolate nanocomposite films reinforced with nanocellulose isolated from oat husk. *International Journal of Biological Macromolecules*. 2016;91:1134-1140.
30. Razali N, Salit MS, Jawaid M, Ishak MR, Lazim Y. A study on chemical composition, physical, tensile, morphological, and thermal properties of roselle fibre: Effect of fibre maturity. *BioResources*. 2015;10(1):1803-1824.
31. Sarki J, Hassan SB, Aigbodion VS, Oghenevweta JE. Potential of using coconut shell particle fillers in eco-composite materials. *Journal of Alloys and Compounds*. 2011;509(5):2381-2385.
32. Satyanarayana KG, Arizaga GG, Wypych F. Biodegradable composites based on lignocellulosic fibers An overview. *Progress in polymer science*. 2009;34(9):982-1021.
33. Segal LGJMA, Creely JJ, Martin Jr AE, Conrad CM. An empirical method for estimating the degree of crystallinity of native cellulose using the X-ray diffractometer. *Textile Research Journal*. 1959;29(10):786-794.
34. Shen Z, Ghasemlou M, Kamdem DP. Development and compatibility assessment of new composite film based on sugar beet pulp and polyvinyl alcohol intended for packaging applications. *Journal of Applied Polymer Science*. 2015;132(4):41354. <https://doi.org/10.1002/app.41354>.
35. Singha AS, Thakur VK. Morphological, thermal, and physicochemical characterization of surface modified pinus fibers. *International Journal of Polymer Analysis and Characterization*. 2009;14(3):271-289. <https://doi.org/10.1080/10236660802666160>.
36. Sofla MRK, Brown RJ, Tsuzuki T, Rainey TJ. A comparison of cellulose nanocrystals and cellulose nanofibres extracted from bagasse using acid and ball milling methods. *Advances in Natural Sciences: Nanoscience and Nanotechnology*. 2016;7(3):035004. <http://dx.doi.org/10.1088/2043-6262/7/3/035004>.
37. Sonia A, Dasan KP. Barrier properties of celluloses microfibrils (CMF)/ethylene-co-vinyl acetate (EVA)/composites. *Composite Interfaces*. 2014;21(3):233-250. <https://doi.org/10.1080/15685543.2014.856644>.
38. Sudharsan K, Mohan CC, Babu PAS, Archana G, Sabina K, Sivarajan M, *et al.* Production and characterization of cellulose reinforced starch (CRT) films. *International Journal of Biological Macromolecules*. 2016;83:385-395.
39. Sun CC. True density of microcrystalline cellulose. *Journal of Pharmaceutical Sciences*. 2005;94(10):2132-2134.
40. Tawakkal ISM, Talib RA, Abdan K, Ling CN. Mechanical and physical properties of kenaf-derived cellulose (KDC)-filled polylactic acid (PLA) composites. *BioResources*. 2012;7(2):1643-1655.
41. Teacă CA, Bodîrlău R, Spiridon I. Effect of cellulose reinforcement on the properties of organic acid modified starch microparticles/plasticized starch bio-composite films. *Carbohydrate polymers*. 2013;93(1):307-315.
42. Thakur VK, Thakur MK, Gupta RK. Raw natural fiber-based polymer composites. *International Journal of Polymer Analysis and Characterization*. 2014;19(3):256-271.
43. Wagh YR, Pushpadass HA, Emerald F, Nath BS. Preparation and characterization of milk protein films and their application for packaging of Cheddar cheese. *Journal of Food Science and Technology*. 2014;51(12):3767-3775.
44. Wu JS, Ho HO, Sheu MT. A statistical design to evaluate the influence of manufacturing factors on the material properties and functionalities of microcrystalline cellulose. *European Journal of Pharmaceutical Sciences*. 2001;12(4):417-425.